Cent. Eur. J. Phys. • 9(2) • 2011 • 438-445
DOI: 10.2478/s11534-010-0144-3

VERSITA

Central European Journal of **Physics**

Polar nanoregions in $Pb(Mg_{1/3}Nb_{2/3})O_3$ (PMN): insights from a supercell approach

Research Article

Eriks Klotins[1]*, Anatoli I. Popov[1,2], Vladimir Pankratov[1], Liana Shirmane[1], Davis Engers[1]

1 *Institute of Solid State Physics, University of Latvia, 8 Kengaraga Str., Riga, LV-1063, Latvia*

2 *Institute Laue-Langevin, BP 156, 38042 Grenoble Cedex 9, France*

Received 5 July 2010; accepted 3 January 2011

Abstract: We report construction of a model of polar nanoregions in the PMN relaxor ferroelectric based on first-principles lattice dynamics for chemically ordered supercells [S.A. Prosandeev et al., Phys. Rev. B 70, 134110 (2004)], combined with invariance under permutations and dipole-dipole interaction as a source supporting randomly oriented residual polarization. Representative analytical estimates of polar nanoregion – supercell mapping reproduce both nonzero local and zero macroscopic polarization of the structure, as well as the temperature change of the supercell anisotropy at cooling and field cooling.

PACS (2008): 71.55.Jv, 77.80.Jk

Keywords: relaxor • ferroelectrics • supercells

1. Introduction

Polar nanoregions play a central role in models of relaxor ferroelectrics characterized by chemical disorder on the microscopic scale supporting ultra-high parameters in technological applications. Experiments have long suggested that typical macroscopic characteristics distinguishing the relaxor ferroelectrics include anomalies in the optic index of refraction [1], the frequency dependence of the peak dielectric constant, and no evidence of macroscopic spontaneous polarization at zero-field cooling, as systematized in [2, 3].

*E-mail: klotins@cfi.lu.lv

Microscopic mechanisms leading to an appearance of these anomalies in relaxor ferroelectrics differ considerably from the phonon picture of conventional, translationally invariant ferroelectrics (with spontaneous and switchable polarization as the defining property) and are interpreted as interplay between the local polarization in polar nanoregions and compositionally induced random electric fields.

Direct observation of polar nanoregions in PMN [4] reveals both local atomic displacements and medium-range ($\sim$ 5 – 50 Å) ordering with the volume fraction increasing with decreasing temperature and reaching the three-dimensional percolation threshold below $T \sim 200$ K, where the polar nanoregions start to overlap and freeze into the polar glass state.

The following prototypes advanced for the description

of relaxor ferroelectrics are $Pb(Sc_{1/2}Nb_{1/2})O_3$ (PSN) and $Pb(Mg_{1/3}Nb_{2/3})O_3$ (PMN) oxides, with polar nanoregions as the key entities.

A great body of approaches attempted within the framework of spin-glass theory [5], random field theory [6], spherical random-bonds/random-fields (SRBRF) model [7], its dynamical version [8], the nanodomain theory of ferroelectric glasses [9], and the model of interacting short-range polar clusters formed by off-center ions [10] contributes greatly to understanding the nature of polar nano-regions supported by chemical and polar disorder.

Spin-glass theory [5] is derived under the presumption of off-center ions and associated randomly oriented dipoles, as well as compositionally induced, random fields as the key entities. At low temperatures local polar regions occur, presumably supported by dipole-dipole interaction, and the system is in a polar-glass state. At finite temperatures the relative number of dipoles whose energy exceeds k_BT rapidly decreases and the polar-glass state disintegrates. This scenario is a departure point for more advanced approaches reproducing the features of relaxor ferroelectrics.

Random field theory [6] is based on the Hamiltonian for a lattice of unit cells by imposing the intercell potential and interaction parameter, both presumed as random. Considering the local potential as a constraint and the kinetic energy as absorbed into the thermal bath yields the extended Ising (Pots) model in an external field. However, to reproduce the dielectric response [7], a rich scale of compositionally induced defect centers and local fields are implemented as adjustable parameters, violating the self-consistence of this approach.

Generalization of the random field theory [7] is attained within the framework of the spherical random-bonds/random-fields (SRBRF) model with chemically ordered regions (chemical clusters) and polar clusters (formally defined as three component vectors), consisting of a number of pseudo-cubic unit cells as the key entities [8]. Interaction between chemical clusters is presumed as infinitely ranged and randomly frustrated according to the Gaussian statistics. Dynamic version of the SRBRF model [8] is implemented by Langevin equations, with relaxation time for the reorientation of polar clusters as an adjustable parameter (by the Vogel-Fulcher relationship). The macroscopic regions (polar clusters) are formally characterized by the same microscopic equation of motion, but a different relaxation time. Output of the SRBRF model is a dynamic response on an oscillating electric field, restricted for uniaxial or isotropic problems. A realistic relaxation time distribution, which would be appropriate at all temperatures, was not resolved.

Numerical evidences of a state when the nanoscale ferroelectric order exists in the absence of macroscopic order are found within the framework of the nanodomain theory of ferroelectric glasses [9], witch-dipole impurities, statistically averaged dipole moments, intra- and inter-domain interactions, and the statistics of random fields as the adjustable entities.

The contemporary approach to the polarization dynamics and the formation of polar nanoregions is derived in [10] within a model of interacting, short-range polar clusters formed by off-center ions. The polarization dynamics is controlled (i) by the distribution of cluster reorientation frequencies and (ii) by distribution of local fields as adjustable parameters. As distinct from [6], the approach of [10] is self-consistent and starts with a Hamiltonian accounting for (i) the energy of orientation of randomly distributed off-center ions; (ii) the quenched random field, originated by compositional fluctuations; and (iii) the applied electric field. With appropriate adjustable parameters, this self-consistent, random-field theory joins microscopic and mesoscopic-level phenomena in disordered systems.

However, the empirical character of early parameterized approaches holds no promise for providing chemically-specific information and understanding about the structural and electronic properties of the ferroelectric relaxors.

Reliable atomistic simulations of structural phase transitions in ferroelectrics began with a first-principles, effective Hamiltonian model for conventional perovskite-type ferroelectrics, structured by spatially invariant elementary cells [11, 12]. However, the physics of chemically disordered and/or low-dimensional structures, comprising uncompensated built-in charges is a subject of long-standing interest.

On fundamental grounds the problem is to determine the possible existence, or the eventual absence, of spontaneous polarization, using first-principles techniques with minimum practical approximations, addressed to the property of interest.

In order to have relaxor properties, the crucial condition is that the chemical microstructure should contain ions violating the charge balance of the host ABO_3 primitive unit cells with random electric fields so preventing ferroelectric ordering in favor of the ferroelectric relaxor state.

Pioneering atomistic simulations based on extensions of the effective Hamiltonian [11] include complex oxides modeled in virtual crystal approximation [13] and the connection of the nanodomains with the microscopic structure of the elementary lattice advanced for PSN and PMN in [2].

The relevant effective Hamiltonian is derived from [12], substituting extra terms addressed to local fields sup-

ported by the chemical disorder on B- sites and/or a contribution from any other charged or polar defects.

Molecular dynamics [2] reveal chemical short-range ordering with uniform characteristic length between freezing and Burns temperatures, supporting the view that polar nanoregions are essentially the same as chemically ordered regions. As to the whole system in grain-scale, it may be considered as consisting of nanoscale regions of enhanced polarization and enhanced polar fluctuations in a less polarized and less susceptible host lattice.

The important stage in joint microscopic and mesoscopic level phenomena in disordered systems is mimicking free-standing, zero-dimensional, ferroelectric nano-particles (nanodots) in vacuum, with their internal structure modified by electric charges and an inhomogeneous strain on the surface [14].

One of the most notable results here is that isolated nanodots of ferroelectrics can have a vortex structure for their dipoles that prefer to rotate from elementary cell to cell, pointing along one of the eight pseudo-cubic $[\pm 1 \pm 1 \pm 1]$ directions. Such a vortex does not create any polarization but rather generates a macroscopic toroidal moment. Zero-dimensional ferroelectric nano-particles embedded into a matrix resemble the $A(B'B'')O_3$ cubic dot embedded in a $AB'O_3$ host lattice. They reveal the existence of different ferroelectric, para-electric, toroidal, and mixed phases, with ferroelectric strengths as adjustable parameters [15]. Consequences for ferroelectric relaxors depend on advances in substituting the macroscopic boundary conditions by a solution of the Poisson's problem for all electrostatic interactions in the system as a whole [14, 15].

A particular topic to be determined and understood concerns the $A(B'B'')O_3$ system with two levels of disorder. At the level of elementary lattice the system is chemically disordered, due the difference of ionic charges in B positions. This disorder is presumably violated in chemically ordered polar supercells, yet condensed randomly without a common causal influence. The corresponding grain-scale model, as a limiting case of [2], is applied to presumably ferroelectric supercells in a para-electric host lattice.

In this paper we report construction of a grain-scale model based on previously reported ab initio calculations [16], combined with the statistics of supercells. The charge balance comes by considering the $Pb(Mg_{1/3}Nb_{2/3})O_3$ (PMN) as structured of primary $Pb^{2+}Mg^{2+}O_3^{2-}$ and $Pb^{2+}Nb^{5+}O_3^{2-}$ primitive cells with 2− and 1+ excess charge, respectively. Unlike a five-atoms $A^{2+}B^{4+}O_3^{2-}$ primitive cell for conventional, perovskite ferroelectrics, the charge balance in $Pb(Mg_{1/3}Nb_{2/3})O_3$ is achieved for a $15n$-atom ($n = 1, 2, \ldots$) supercell.

First principles treatment (with the *ab initio* simulation package VASP [16]) of stoichiometric ordered 15-ion supercells [16, 17] yields local 1:2 ordering along the [111] direction and an anti-ferroelectric, $P\bar{3}m1$, reference configuration that is unstable with respect to the lower-energy, structurally stable ferroelectric state, $P1$.

The model assumes that there exists a simulation area, comprising energetically equivalent polar supercells (presumably being the same as in the 15-ion periodic arrangement [16]). Supercells, distinguished by one of eight local polarization vectors supporting zero total polarization, are embedded in a disordered host lattice with no ferroelectric activity. The balance between charges and fields in the simulation area is determined by dipole-dipole interaction between supercells. The initial conditions for polarization meet requirements for zero total polarization over the simulation area and are maintained at high temperature, at which the dipole-dipole interaction turns to zero.

Temperature behavior of local polarization vectors is given by the statistics in the canonical ensemble, determining the local polarization of individual supercells. We give details of this chemically ordered supercell picture in terms of a coarse-grained Hamiltonian and mean field statistics simulations, revealing a change of the supercell anisotropy during cooling as the main result of this study.

The paper is organized as follows. Section 2 describes the coarse-grained Hamiltonian as derived from the polarization of structurally stable states [16], phenomenologically augmented for a simulation area of $8 \times 8 \times 8$ 15-ion supercells. In Section 3, illustrative examples of the temperature change of the supercell anisotropy during cooling and during field cooling is given. The paper closes with a summary (Section 4) and an outlook on future lines of research.

2. Coarse-grained Hamiltonians: definitions and approximations

Bare and total coarse-grained Hamiltonians are distinguished for the system of supercells embedded in the host lattice. The bare Hamiltonian is derived from the results of ionic relaxation of 15-ion chemically ordered supercells [16]. Polarization of the local, structurally stable supercell is presumably the same as found in a periodic system [16]. In this section we start with lattice parameters of a supercell as a=5.682, b=5.759, c=6.964, $\alpha = 89.97$, $\beta = 90.48$, $\gamma = 120.43$, and $\Omega_{cell} = 1.15742 \cdot 10^{-28}$ m^3; and local polarization as $P_x = 0.474$, $P_y = 0.476$, $P_z = 0.016$ C m^{-2} (in Cartesian coordinate frame). All these parameters came from [16]. The Hamiltonian for a bare i-th supercell is given by a low-order Tailor expansion of potential energy $U(Px, Py, Pz)$ in linear, harmonic and anharmonic

terms

$$U(Px, Py, Pz) = \sum_{m,n,k=0}^{\infty} a_{mnk} \tag{1}$$

with expansion coefficients

$$a_{mnk} = \frac{1}{m!n!k!} \frac{\partial^{m+n+k} U\left(P_{x_0}, P_{y_0}, P_{z_0}\right)}{\partial P_x \partial P_y \partial P_z} P_x^m P_y^n P_z^k. \tag{2}$$

The terms linear in polarization are reproduced by the condition $0 < m + n + k \leqslant 1$, which yields

$$\begin{aligned} a_{001} &= P_z U^{(0,0,1)}, \\ a_{011} &= P_y U^{(0,1,0)}, \\ a_{100} &= P_x U^{(1,0,0)}. \end{aligned} \tag{3}$$

The harmonic terms are reproduced by the condition $1 < m + n + k \leqslant 2$ and preserve exclusively the even degrees at polarization

$$\begin{aligned} a_{002} &= \frac{1}{2} P_z^2 U^{(0,0,2)}, \\ a_{020} &= \frac{1}{2} P_y^2 U^{(0,2,0)}, \\ a_{200} &= \frac{1}{2} P_x^2 U^{(2,0,0)}. \end{aligned} \tag{4}$$

The anharmonic terms are reproduced by the condition $3 < m + n + k \leqslant 4$, which yields

$$\begin{aligned} a_{004} &= \frac{1}{24} P_z^4 U^{(0,0,4)}, \\ a_{040} &= \frac{1}{24} P_y^4 U^{(0,4,0)}, \\ a_{400} &= \frac{1}{24} P_x^4 U^{(4,0,0)}. \end{aligned} \tag{5}$$

Equations (1)-(5) constitute the Hamiltonian of a bare supercell as a sum of linear, harmonic, and anharmonic terms

$$H_{eff}^{(b)} = H_{lin} + H_{harm} + H_{anharm}. \tag{6}$$

Here $H_{lin} = a_{001} + a_{010} + a_{100}$, $H_{harm} = a_{002} + a_{020} + a_{200}$ and $H_{anharm} = a_{004} + a_{040} + a_{400}$. It is convenient to write the coarse-grained bare Hamiltonian in Ginzburg-Landau form by following the denominations $U^{(0,0,1)} \to -\lambda_z$, $U^{(0,1,0)} \to -\lambda_y$, $U^{(1,0,0)} \to -\lambda_x$, $U^{(0,0,2)} \to -\alpha_z$, $U^{(0,2,0)} \to -\alpha_y$, $U^{(2,0,0)} \to -\alpha_x$, $U^{(0,0,4)} \to -\beta_z$, $U^{(0,4,0)} \to -\lambda_y$, and $U^{(4,0,0)} \to -\beta_x$.

With these denominations the Hamiltonian Eq. (6) reads as follows

$$\begin{aligned} H_{eff}^{(b)} = &- \frac{\alpha_x P_x^2}{2} - \frac{\alpha_y P_y^2}{2} - \frac{\alpha_z P_z^2}{2} \\ &+ \frac{\beta_x P_x^4}{24} + \frac{\beta_y P_y^4}{24} + \frac{\beta_z P_z^4}{24} \\ &- \lambda \cdot \mathbf{P} - \mathbf{L} \cdot \mathbf{P} \end{aligned} \tag{7}$$

with linear, λ, harmonic, α, anharmonic, β, and external field, $\mathbf{L}$, terms. The coefficients α, β, λ in Eq. (7) are found from the minimum-energy constraint

$$\frac{\partial H}{\partial \mathbf{P}} = 0.$$

As a crucial ingredient that makes the model solvable, we exclude the metastability by setting the discriminant of the minimum-energy relation positive as

$$-8\alpha_\alpha^3 + 9\beta_\alpha \alpha_\alpha^2 = \varepsilon \beta_\alpha^3,$$

($\alpha = x, y, z$ are Cartesian coordinates and ε is an infinitesimal positive constant). The third constraint is based on the estimates of energy

$$E_b = |\mathbf{P}|^2 \Omega_{cell} (2\varepsilon_\infty \varepsilon_0)^{-1}$$

that (on physical grounds) must be commensurable with thermal energy $E_t = k_b T$. At Burns temperature $T_B \approx 650$ K, the condition $E_t = E_B$ gives a rough estimate for the factor between the energy assigned to a bare supercell and its polarization square as

$$C_c = \Omega_{cell} (2\varepsilon\varepsilon_0)^{-1} = 1.98 \cdot 10^{-20} \text{ m}^4 \text{ V/C}.$$

Finally, the third constraint is determined by the energy of particular components of polarization as

$$-\frac{\alpha_\alpha P_\alpha^2}{2} + \frac{\beta_\alpha P_\alpha^4}{24} - \lambda_\alpha P_\alpha = -C_c P_\alpha^2, \tag{8}$$

where P_α are results from first principles [16].

Table 1. Expansion coefficients of the energy landscape reproducing the first-principles polarization. Dimensions are J/C in appropriate degrees. Values of expansion coefficients are rather illustrative due the ambiguous results for polarization in PMN [17].

$\lambda = \{\lambda_x, \lambda_y, \lambda_z\}$	α_x	α_y	α_z	β_x	β_y	β_z
$\left\{\begin{array}{l} 6.27684\times10^{-21}, \\ 6.27684\times10^{-21}, \\ 2.11876\times10^{-22} \end{array}\right\}$	3.97268×10^{-20}	3.97268×10^{-20}	3.97268×10^{-20}	1.41455×10^{-18}	1.40268×10^{-18}	1.24146×10^{-15}

The system $A(B'B'')O_3$ as a whole is chemically disordered at the level of elementary lattices. The underlying physics is chemical disorder supporting random fields due the difference of ionic charges in B-positions. However, this disorder is presumably violated in chemically ordered supercells, condensed randomly without common causal influence as formally implemented by invariance of supercells under permutations. The consequence is 8 energetically equivalent varieties of local polarization vectors, specified by Miller indices $[\bar{1}\,\bar{1}\,\bar{1}], [\bar{1}\,\bar{1}\,1], [\bar{1}\,1\,\bar{1}], [\bar{1}\,1\,1], [1\,\bar{1}\,\bar{1}], [1\,\bar{1}\,1], [1\,1\,\bar{1}]$, and $[1\,1\,1]$. Here the symmetric indices are related to the opposite polarization. The local polarization for individual supercells is distinguished by local polarization vectors **LP** corresponding to the aforementioned Miller indices as **LP**1$[\bar{1}\,\bar{1}\,\bar{1}]$, **LP**2$[\bar{1}\,\bar{1}\,1]$, **LP**3$[\bar{1}\,1\,\bar{1}]$, **LP**4$[\bar{1}\,1\,1]$, **LP**5$[1\,\bar{1}\,\bar{1}]$, **LP**6$[1\,\bar{1}\,1]$, **LP**7$[1\,1\,\bar{1}]$, **LP**8$[1\,1\,1]$.

For the simulation area comprising $8\times8\times8 = 512$ supercells each variety of local polarization vectors (**LP**$[i][^*], i = 1,\ldots,8$) repeats itself 64 times. Because each supercell should have condensed randomly, the simulation area consists of spatially random **LP**'s, and its sequence is formally found by random permutation. Finally, each supercell is set at coordinates $\{x_i, y_i, x_i\}$ for $i = 1, 2, \ldots, 512$ sites of the simulation area and determines the initial conditions for the temperature behavior while cooling.

Considering the supercells as embedded in the disordered host lattice with no ferroelectric activity and distinguished by dielectric permittivity ε_∞, the dipole-dipole interaction between supercells is given by

$$H_i^{dip} = \left[\frac{1}{2}\left(\frac{1}{4\pi\varepsilon_0}\right)\frac{1}{\varepsilon_\infty}\frac{\Omega_{cell}^2}{S_{cell}^3}\right] \sum_{j=1}^{j_{max}} \frac{\mathbf{P}_i\cdot\mathbf{P}_j - 3\left(\mathbf{e}_{ij}\cdot\mathbf{P}_i\right)\left(\mathbf{e}_{ij}\cdot\mathbf{P}_j\right)}{R_{ij}^3}. \quad (9)$$

Here $\mathbf{R}_i, \mathbf{R}_j$ are Cartesian coordinates of selected and interacting supercells, respectively. $R_{ij} = |\mathbf{R}_i - \mathbf{R}_j|$ is the Euclidean distance between supercells, and

$$\mathbf{e}_{ij} = \frac{\mathbf{R}_{ij}}{|\mathbf{R}_{ij}|}$$

is the unit vector parallel to the line joining the centers of two supercells [18]. The location of supercells is supposed at sites $\{x_i, y_i, z_i\}$ with S_{cell} spacing equal to the mean value of its presumably random distribution.

It must be emphasized that the simulation area is organized by random distribution of a finite number of supercells undergoing dipole-dipole interaction, factorized by the optical dielectric constant of the host lattice, and emerges neither nonzero averaged (spontaneous) polarization nor surface effects.

At finite temperatures the dipole-dipole sums over neighboring supercells (indexed by j) are preceded within the mean-field approach by replacing the polarization of j-th supercells with the initial (or previous) values of polarization. The dipole-dipole interaction contributes in the Hamiltonian Eq. (7) by a field-like term $\lambda\cdot\mathbf{P}_i$, reducing evaluation of the first moment to a threefold numerical integration.

In subsequent illustrative examples the estimates of supercell spacing $S_{cell} = 10^{-9}$ m, and the optical dielectric constant of the host lattice $\varepsilon_\infty = 10$ [2] both contribute in the dipole-dipole interaction factor (the term in square brackets in Eq. (2)) as $6.011504\cdot10^{-21}$ Vm^4C^{-1}. The total (coarse-grained) Hamiltonian for the i-th supercell is given by $H_i = H_i^{loc} + H_i^{dpl}$.

3. Statistics of supercells

For the total Hamiltonian

$$H^{tot} = \sum_i \left(H_i^{loc} + H_i^{dip}\right)$$

the multivariate probability density involves statistics in the canonical ensemble [19]

$$\rho\left[\{\mathbf{P}_i; \mathbf{P}_j\}\right] \equiv \exp\left[-\widetilde{\beta}H^{tot}\right], \quad (10)$$

where the inverse temperature is defined as

$$\widetilde{\beta} \equiv \frac{1}{k_B T},$$

with the Boltzmann's constant k_B. The expectation value of polarization [19] reads as

$$E(P_x) = \int P_x \rho\left(P_x, P_y, P_z\right) dP_y P_z \qquad (11)$$

and similar relations for $E\left(P_y\right), E\left(P_z\right)$. Integration of Eqs. (11) is started at high temperatures and proceeds within the mean field approach. The unknown polarization $\mathbf{P}_j$ is replaced by the corresponding values of the initial conditions or, subsequently, by the values found over the preceding temperature step. Within the framework of this approach the temperature is sequentially decreased, step by step, from Burns temperature ($\approx$ 650 K [1, 20, 21]), estimated as low enough for chemical ordering and high enough to ignore the dipole-dipole interaction between supercells.

At each temperature step, the polarization obtained from the previous simulation is used as the starting point for the next one, including the impact of the instant dipole-dipole interaction, and so evolving the system down to 10 K.

It must be emphasized that the current supercell approach is a limiting case of [2]. This is reasonable below the temperature at which polar nanoregions emerge in the host lattice distinguished by permittivity, and above the temperature at which pre-transition phenomena appear supported by competing polar and chemical correlations [22]. Temperature development of the system is illustrated in Fig. 1 by P_x and P_y plots.

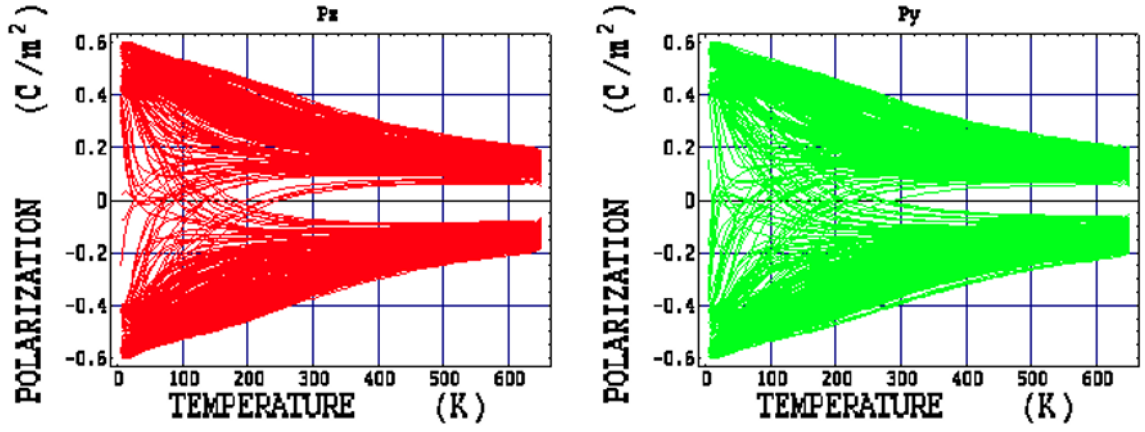

Figure 1. Temperature change of the supercell anisotropy for all supercells in the simulation area: polarization P_x (left picture, red online) and P_y (right picture, green online). At high temperature the initial polarization of each supercell approaches zero, maintaining the number of supercells belonging to one of the eight available local polarization vectors LP. During cooling the polarization of individual supercells either increases, with the LP maintained, or undergoes a temperature change of the supercell anisotropy toward the opposite LP. Symmetry of polarization plots with respect to the zero polarization line implies zero total polarization.

The impact of the external field evolves linearly as the $\mathbf{L}\cdot\mathbf{P}$ term in Eq. (7). For the external field $L_x = 5.16 \cdot 10^7$ V/m (estimated as large in comparison with the impact of the dipole interaction equivalent to $2.6 \cdot 10^7$ V/m) is illustrated in Fig 2.

At high temperature (Fig. 2) each of 8 available **LP** is assigned to an equal number of 64 supercells. Under an external field $E_x > 0$ the supercells **LP**1$[\bar{1}\,\bar{1}\,\bar{1}]$, **LP**2$[\bar{1}\,\bar{1}\,1]$, **LP**3$[\bar{1}\,1\,\bar{1}]$, **LP**4$[\bar{1}\,1\,1]$, having initial state polarization $P_x < 0$, is aligned along the field, and their amount decreases to about $4 \times 37 = 148$, constituting the first family (lower in Fig. 2). The number of supercells **LP**5$[1\,\bar{1}\,\bar{1}]$, **LP**6$[1\,\bar{1}\,1]$, **LP**7$[1\,\bar{1}\,\bar{1}]$, and **LP**8$[1\,1\,1]$ all having initial state polarization $P_x > 0$, is not changed under an external field. However, about $4 \times 27 = 108$ supercells flipped from the state $P_x < 0$ to state $P_x > 0$. As a result, the second family of about $4 \times 85 = 340$ supercells (upper in Fig. 2) appears to prevail over the first family of 148

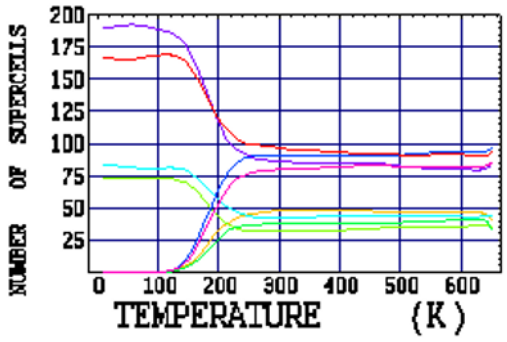

Figure 2. Plots of the temperature dependence for the varieties of local polarization vectors entangled during field cooling. At 300 K the sequence of local polarization vectors is LP8[1 1 1] (red), LP5[1 $\bar{1}$ $\bar{1}$] (light blue), LP6[1 $\bar{1}$ 1] (plum), LP7[1 $\bar{1}$ $\bar{1}$] (pink), LP1[$\bar{1}$ $\bar{1}$ $\bar{1}$] (gold), LP4[$\bar{1}$ 1 1] (turquoise), LP3[$\bar{1}$ 1 $\bar{1}$] (sea green), and LP2[$\bar{1}$ $\bar{1}$ 1] (bright green).

supercells. During cooling below $\sim$ 250 K (in the scale of Fig. 2), the dipole-dipole interaction comes into play, and each of the lower/upper families of supercells undergoes subsequent splitting. Successive saturation at the end of cooling yields the number of **LP** with $P_x > 0$ prevailing over $P_x < 0$, as expected on physical grounds.

4. Summary

We report the construction of a model of polar nanoregions in the PMN relaxor ferroelectric, inspired by first-principles lattice dynamics for chemically ordered supercells [16, 17] and phenomenologically augmented by coarse-grained Hamiltonian. Approaches in the derivation of the model are summarized as follows:

1. The PMN relaxor ferroelectric is modeled by polar nanoregions embedded in the disordered host lattice with no ferroelectric activity.

2. Polar nanoregions are assigned to previously reported, chemically ordered supercells specified by lattice parameters and residual polarization.

3. The disordered host lattice is specified by dielectric permittivity factorizing the dipole-dipole interaction between supercells.

4. The bare supercell is specified by a coarse-grained Hamiltonian represented by low-order Tailor expansion in linear, harmonic, and anharmonic terms; this is presumably adequate for models with negligible mode-mode interaction in the phonon picture.

5. The simulation area consists of polar supercells supporting zero macroscopic polarization.

6. The temperature dependence is solved within the mean-field approach. This is reasonable below the temperature at which polar nanoregions emerge in the host lattice and above the temperature at which pre-transitional phenomena appear.

These approximations help to explain the role of energetically equivalent structural varieties of the supercells and their invariance under permutations as a source supporting randomly oriented residual polarization, without adjustable parameters like random intracell and intercell interactions and quenched electric fields.

Temperature evaluation within the mean-field approximation qualitatively reproduces experimental evidences of local polarization approaching zero at high temperatures and the change of the supercell anisotropy at medium temperatures, with zero total polarization maintained. Nonzero total polarization is reproduced in the course of field cooling.

The emphasis in this model is still very much on the view that polar nanoregions are essentially the same as chemically ordered regions and, as a consequence, the volume fraction of polar nanoregions correlates with the chemical ordering and is invariant with respect to temperature. Reasonable questions not fully understood and answered within the chemically ordered supercell picture include the increase of the volume fraction of polar nanoregions with decreasing temperature and the pre-transitional phenomena (interpreted as percolation threshold [4] or glassy freezing [22]) evidenced below some critical temperature by the pair distribution function [4] and NMR spectra [22]. Pre-transitional phenomena are definitely incompatible with the supercell picture and raise the problem of more complete first-principles and time-dependent molecular dynamics simulations [23].

As to the high temperature region, there are experimental evidences [24] revisiting the Burns temperature at about 420 K that activates unresolved problems for the theory of short-range polar correlations beyond the supercell approach.

A complementary technique is to look at the nonlinearity of intersite potential as an ingredient of the dynamical interpretation of polar nanoregions. Indeed, the nonlinear intersite potential, if supplemented by linear (dipole-dipole) interaction and momentum terms, results in intrinsic localized excitations within a well developed framework of modulation instability and grand-canonical statistics. Preliminary evaluations [25] reveal a remarkable property – the chemical disorder favors a spontaneous dipole moment and suggests a possible pathway to observation-matching answers to those questions.

Acknowledgements

This work was supported by the Latvian State research program, Project #2 and ESF project Nr. 2009/0202/1DP/1.1.1.2.0/09/APIA/VIAA/141.

References

[1] G. Burns, F.H. Dacol, Solid State Commun. 48, 853 (1983)
[2] B.P. Burton et al., Phase Transit. 79, 91 (2006)
[3] J. Macutkevic et al., Phys. Rev. B 74, 104106 (2006)
[4] I.K. Jeong et al., Phys. Rev. Lett. 94, 147602 (2005)
[5] B.E. Vugmeister, M.D. Glinchuk, Rev. Mod. Phys. 62, 993 (1990)
[6] H. Qian, L.A. Bursil, Int. J. Mod. Phys. B 10, 2027 (1996)
[7] R. Pirc, R. Blinc, Phys. Rev. B 60, 13470 (1999)
[8] R. Pirc, R. Blinc, V. Bobnar, Phys. Rev. B 63, 054203 (2001)
[9] A.E. Maslennikov, S.A. Posandeev, V.S. Vikhin, S.E. Kaphan, Integr. Ferroelectr. 38, 153 (2001)
[10] B.E. Vugmeistar, Phys. Rev. B 73, 174117 (2006)
[11] R.D. King-Smith, D. Vanderbilt, Phys. Rev. B 49, 5828 (1994)
[12] W. Zhong, D. Vanderbilt, K.M. Rabe, Phys. Rev. B 52, 6301 (1995)
[13] L. Belaiche, A. Garcia, D. Vanderbilt, Phys. Rev. Lett. 84, 5427 (2000)
[14] I.I. Naumov, L. Belaiche, H. Fu, Nature 432, 737 (2004)
[15] S. Prosandeev, L. Bellaiche, Phys. Rev. Lett. 97, 167601 (2006)
[16] S.A. Prosandeev et al., Phys. Rev. B 70, 134110 (2004)
[17] N. Choudhury, Z. Wu, E.J. Walter, R.E. Cohen, Phys. Rev. B 71, 125134 (2005)
[18] W. Zong, D. Vanderbilt, K.M. Rabe, Phys. Rev. Lett. 73, 1861 (1994)
[19] N.G. Van Kampen, Stochastic processes in Physics and Chemistry, Fifth impression (Elsevier, Amsterdam, 2004)
[20] D. Vieland, J. Li, S. Jang, L.E. Cross, Phys. Rev. B 43, 8316 (1991)
[21] N. Takesue, Y. Fujii, H. You, Phys. Rev. B 64, 184112 (2001)
[22] R. Blinc, V. Laguta, B. Zalar, Phys. Rev. Lett. 91, 247601 (2003)
[23] Y. Liu, D.A. Yarne, M.E. Tuckerman, Phys. Rev. B 68, 125110 (2003)
[24] P.M. Gehring et al., Phys. Rev. B 79, 224109 (2009)
[25] E. Klotins, Physica E 42, 614 (2010)